

## Observation of the Drift Wave Instability in Bounded ECR Plasma

K. Kamataki<sup>1</sup>, Y. Nagashima<sup>2</sup>, S. Shinohara<sup>1</sup>, Y. Kawai<sup>2</sup>, M. Yagi<sup>2</sup>, K. Itoh<sup>3</sup>, S. -I. Itoh<sup>2</sup>

<sup>1</sup> *Interdisciplinary Graduate School of Engineering Science, Kyushu University,*

*Kasuga, Fukuoka 816-8580, Japan*

<sup>2</sup> *Research Institute for Applied Mechanics, Kyushu University,*

*Kasuga, Fukuoka 816-8580, Japan*

<sup>3</sup> *National Institute for Fusion Science, Toki, Gifu 509-5292, Japan*

### 1 INTRODUCTION

The plasma turbulence and its role in anomalous transport are crucial issues in high temperature plasma physics. The nonlinear self-regulation mechanism of drift wave turbulence has been subject to attentions in order to clarify the structural formation of plasma turbulence [1]. The drift wave is well known as a low frequency instability driven by a pressure gradient transverse to the magnetic field [2]. The drift wave instability has been extensively studied in linear magnetized plasmas with different plasma parameter regimes. The theoretical analysis has revealed that the growth rate of collisional drift instability is proportional to electron-ion collision frequency. However, in weakly ionized plasma, the ion - neutral particle collisions cannot be neglected. We will show both experimentally and theoretically that this effect influences the growth rate of drift wave instability.

In this paper, we investigate the excitation on drift wave instability in bounded linear Electron Cyclotron Resonance (ECR) plasma device [3]. A coaxial waveguide is installed to achieve a steep density gradient in the radial direction. The axial boundary condition is determined by metals on both ends of the device. The transition from drift mode to flute mode was observed by varying filling pressure. Conditions, for which drift and flute modes coexist, were identified. We then study the dependence of the growth rate  $\gamma$  of collisional drift-interchange (flute) instability on ion-neutral collision frequency  $\nu_{in}$  using Hasegawa-Wakatani model [4]. The result explains the experimental observation on filling gas pressure.

### 2 EXPERIMENTAL APPARATUS

The schematic diagram of the ECR plasma device (inner diameter *i.d.* is 400 mm and axial length  $L$  is 1200 mm) is shown in Fig. 1 (a). The axial magnetic field profile is shown in Fig. 1 (b). Typical plasma parameters were: electron density  $n_e \sim 10^{17} \text{ m}^{-3}$  and electron temperature  $T_e \sim 2 \text{ eV}$ . The ionization rate was on the order of a few % (weakly ionized

plasma). The chamber was evacuated to  $1.0 \times 10^{-7}$  Torr, and then argon gas was introduced into the chamber at a pressure  $P(\text{Ar})$  of  $(0.1 - 2.0) \times 10^{-3}$  Torr. Radial density and potential profiles and their plasma fluctuations were measured by Langmuir probes under the various conditions. ECR plasma was produced by launching a microwave with the frequency of 2.45 GHz through a coaxial waveguide (*i.d.* = 100 mm and  $L = 210$  mm). Input microwave power  $P_\mu$  was 200 - 500 W. By using this small diameter waveguide, the strong radial gradient in density was formed. In addition, the axial boundary condition was determined by metals on both ends of the vacuum chamber.

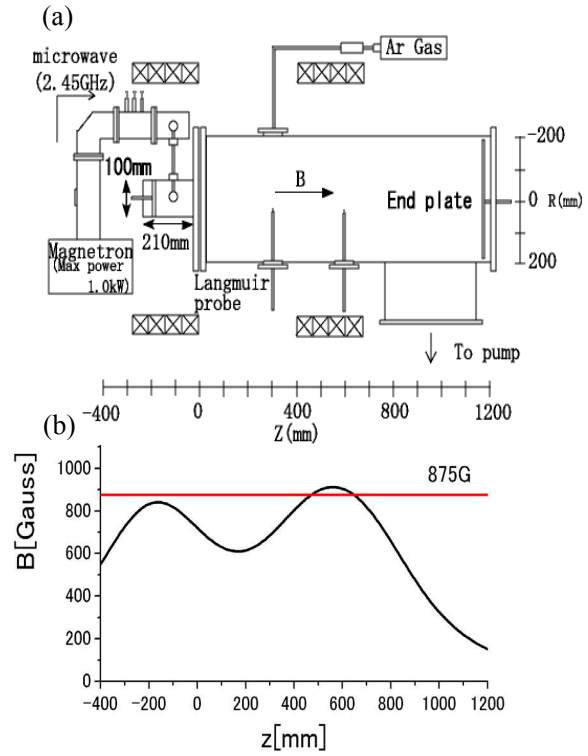


Fig. 1 (a) Schematic diagram of the experimental setup and (b) axial magnetic field profile

### 3 Hasegawa-Wakatani Model

Hasegawa-Wakatani model (with the effect of ion-neutral collision and equivalent gravitational acceleration  $g$  by the bad magnetic curvature) is utilized, in order to study the dependence of the growth rate of collisional drift-interchange instability on ion-neutral collision frequency. In this analysis, the local dispersion relation is evaluated. The magnetic field is specified to lie along the  $z$  axis, and the density gradient to be along the  $x$  axis. The azimuthal direction is the  $y$  axis. The equations governing the instability are vorticity Eq. (1) and continuity Eq. (2).

$$\frac{\partial}{\partial t} \nabla_{\perp}^2 \phi = -v_{in} \nabla_{\perp}^2 \phi + C(\phi - n) - g \frac{\partial n}{\partial y} \quad (1)$$

$$\frac{\partial}{\partial t} n + \kappa \frac{\partial \phi}{\partial y} = g \frac{\partial}{\partial y} (\phi - n) + C(\phi - n) \quad (2)$$

Here,  $C = m_i k_{\parallel} / m_e v_e$ ,  $\kappa = -dn / dr$ ,  $\phi$  is the electrostatic potential,  $v_e$  is sum of the electron-ion and electron-neutral collision frequencies ( $v_e = v_{ei} + v_{en}$ ),  $v_{in}$  is the ion-neutral collision frequency and  $\Omega_i$  is the ion cyclotron angular frequency. In Eqs. (1) and (2) the following normalization is done:  $\Omega_i t \rightarrow t$ ,  $r / \rho_s \rightarrow r$ ,  $n / n_0 \rightarrow n$ ,  $e \phi / T_e \rightarrow \phi$ . Substituting

the Eq. (1) into the Eq. (2) and assuming  $k_{\parallel} \rightarrow 0$  and  $k_{\perp} \approx k_y$ , we have

$$\omega = \frac{gk_y \pm \sqrt{g^2 k_y^2 - 4g\kappa}}{2} \Rightarrow \gamma \propto \sqrt{g\kappa} \quad (3)$$

which represents the dispersion relation of flute wave instability ( $\gamma$ : growth rate). On the other hand, assuming  $g \rightarrow 0$  and  $k_{\perp} \ll 1$ , we have

$$\omega = \frac{-iC \pm \sqrt{4iCk_{\perp}^2 k_y \kappa - C^2}}{2k_{\perp}^2} \Rightarrow \gamma \propto \frac{k_y \kappa}{C} \propto v_e \quad (4)$$

which shows the relation of the drift wave instability.

## 4 EXPERIMENTAL AND NUMERICAL RESULTS

### 4.1 Fluctuation measurements

A typical power spectrum of the ion saturation current measured in the ECR plasma is shown in Fig. 2. The frequency spectrum of ion saturation current is characterized by the presence of two intense peaks of the frequencies  $f$  of  $\sim 1.5$  and  $\sim 4.3$  kHz. The axial wave number, the direction of azimuthal propagation and phase difference between density and potential fluctuations were measured with Langmuir probes aligned azimuthally and axially. From the measurement results, fluctuations at  $f \sim 1.5$  and

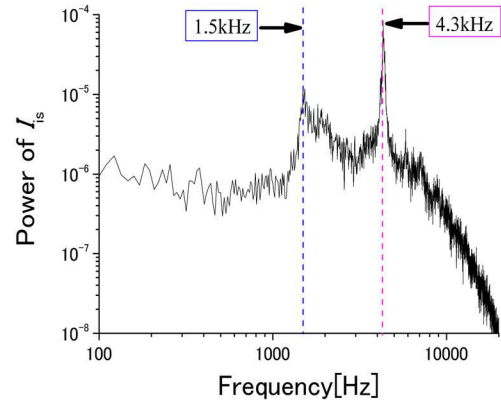


Fig. 2 Frequency spectrum of the ion saturation current ( $z = 300$  mm,  $r = 27$  mm,  $P(\text{Ar}) = 1.0 \times 10^{-3}$  Torr,  $P\mu = 300$  W and  $B = 685$  Gauss).

4.3 kHz were the flute and the drift wave instabilities, respectively [5]: As to the fluctuation of  $f \sim 1.5$  kHz, a phase difference between density and potential fluctuation was  $50 \sim 80^\circ$  and the axial mode number was  $n \sim 0$ . On the other hand, as to the fluctuation of  $f \sim 4.3$  kHz, the phase difference was  $\sim 40^\circ$  and  $n \sim 1 - 2$  ( $k_{\parallel} = n\pi / L$ , i.e.,  $n = 1$  indicates that the half wavelength is the same as the device length  $L$ ). Both frequencies were much smaller than the ion cyclotron frequency  $f_{ci} \sim 26$  kHz.

### 4.2 Gas pressure dependence

Figure 3 shows the plot of the square of amplitude of the drift wave instability ( $f \sim 4.3$  kHz) and flute instability ( $f \sim 1.5$  kHz) as a function of gas pressure. Drift wave was observed at low filling-pressure,  $P(\text{Ar}) = (0.4 \sim 1.6) \times 10^{-3}$  Torr. Flute wave was observed at higher filling pressure,  $P(\text{Ar}) = (1.0 \sim 2.0) \times 10^{-3}$  Torr. Furthermore, two modes were coexistent in a

range of  $P(\text{Ar}) = (1.0 \sim 1.6) \times 10^{-3}$  Torr.

Relationship between  $\gamma$  and  $v_{\text{in}}$  is shown in Fig. 4, where  $\gamma$  was calculated using the Hasegawa-Wakatani model. In this figure,  $(m,n) = (1,1)$  and  $(m,n) = (1,0)$  show the drift wave instability and flute one, respectively. Figure 4 shows that as  $v_{\text{in}}$  increases,  $\gamma$  of the drift wave instability decreases. That is,  $v_{\text{in}}$ , which is proportional to  $P(\text{Ar})$ , plays an important role in the stabilization of the drift wave. The comparison between Figs. 3 and 4 indicates that the coexistence of the  $n = 1$  mode (drift wave instability) and the  $n = 0$  mode (flute instability) is qualitatively understood.

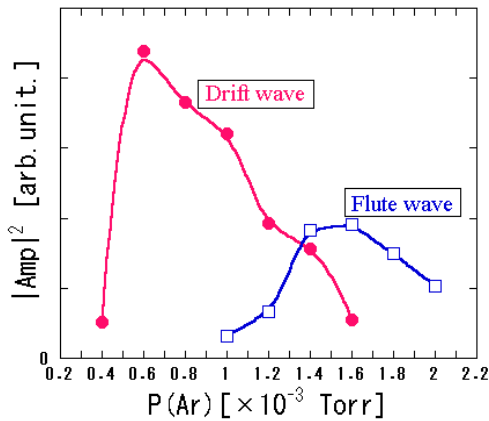


Fig. 3 Pressure dependence of the square of amplitude of drift wave instability and flute instability ( $z = 300$  mm,  $r = 27$  mm,  $P\mu = 300$  W and  $B = 685$  Gauss).

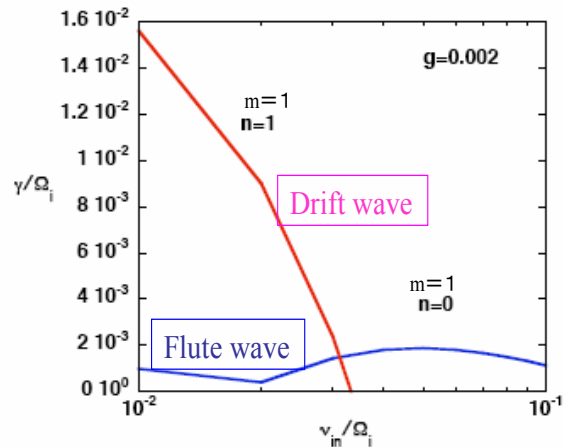


Fig. 4 Relationship between  $\gamma$  and  $v_{\text{in}}$ , where  $\gamma$  is calculated using the Hasegawa-Wakatani model.

## 5 CONCLUSIONS

In the ECR plasma device, the drift wave instability was excited by imposing boundary conditions in the radial and axial direction. We observed the coexistence of the drift and flute wave instabilities. Moreover, the coexistence of two modes qualitatively agreed well with the numerical analysis by the Hasegawa-Wakatani model. The present result suggests that ion-neutral collisions, which are proportional to gas pressure, play an important role in the excitation and stabilization of the drift wave instability: comparatively weak ion-neutral collisions lead to excite the drift instability. Nonlinear interactions between co-existing drift and flute modes will be studied. This work is partly supported by Specially Promoted Research Project (16002005).

## REFERENCES

- [1] P. H. Diamond, S.-I. Itoh, K. Itoh and T. S. Hahm, Plasma Phys. Control. Fusion **47**, 5 (2005).
- [2] W. Horton, Rev. Mod. Phys **71**, 735 (1999).
- [3] M. Koga and Y. Kawai, Phys. Plasmas **10**, 650 (2003).
- [4] H. Sugama, M. Wakatani and A. Hasegawa, Phys. Fluids **31**, 1601 (1988).
- [5] D. L. Jassby, Phys. Fluids **15**, 1590 (1972).